Magnetic nanostructures for marine and freshwater toxins removal

Jesús M. González-Jartín [a], Lisandra de Castro Alves [b], Amparo Alfonso [a], Y. Piñeiro [b], Susana Yáñez Vilar [b], Inés Rodríguez [a,c] , Manuel González Gomez [b], Zulema Vargas Osorio [b], María J. Sainz [d], Mercedes R. Vieytes [d], J. Rivas [b*], Luis M. Botana [a*].

[a]Departamento de Farmacología, Facultad de Veterinaria, Universidade de Santiago de Compostela, 27002, Lugo, Spain.
[b]Departamento de Física Aplicada, Universidad de Santiago de Compostela, Facultad de Física, 15782, Santiago de Compostela, Spain.
[c]Laboratario CIFGA S.A., Avda. Benigno Rivera, 56, 27003, Lugo, Spain.
[d]Departamento de Producción Vegetal y Proyectos de Ingeniería, Facultad de Veterinaria, Universidade de Santiago de Compostela, 27002, Lugo, Spain.
[e]Departamento de Fisiología, Facultad de Veterinaria, Universidade de Santiago de Compostela, 27002, Lugo, Spain.

Jesús M. González-Jartín: jesus.gonzalez@usc.es
Lisandra de Castro Alves: lisandracristina.decastro@usc.es
Amparo Alfonso: amparo.alfonso@usc.es
Y. Piñeiro: y.pineiro.redondo@usc.es
Susana Yáñez Vilar: susana.yanez@usc.es
Inés Rodríguez: ines.rodriguez@cifga.com
Manuel González Gomez: manuelantonio.gonzalez@usc.es
Zulema Vargas Osorio: zulema.vargas@usc.es
M. J. Sainz: mj.sainz@usc.es
M. R. Vieytes: mmercedes.rodriguez@usc.es
J. Rivas: jose.rivas@usc.es
Luis M. Botana: luis.botana@usc.es

* Corresponding author:
Luis M. Botana
Tfn: + 34 982 822 233
Fax: + 34 982 822 233
E-mail: luis.botana@usc.es

* Alternative corresponding author:
Jose Rivas
Tfn: + 34 881813062
Fax: + 34 881814112
E-mail: jose.rivas@usc.es

Abstract

Marine and freshwater toxins contaminate water resources, shellfish and aquaculture products, causing a broad range of toxic effects in humans and animals. Different core-shell nanoparticles were tested as a new sorbent for removing marine and freshwater toxins from liquid media. Water solutions were contaminated with 20 µg/L of marine toxins and up to 50 µg/L of freshwater toxins and subsequently treated with 250 or 125 mg/L of nanoparticles. Under these conditions, carbon nanoparticles removed around 70% of saxitoxins, spirolides, and azaspiracids, and up to 38% of diarrheic shellfish poisoning toxins. In the case of freshwater toxins, the 85% of microcystin LR was eliminated, other cyclic peptide toxins were also removed in a high percentage. Marine toxins were adsorbed in the first five min of contact, while for freshwater toxins it was necessary 60 min to reach the maximum adsorption. Toxins were recovered by extraction from nanoparticles with different solvents. *Gymnodinium catenatum*, *Prorocentrum lima*, and *Microcystis aeruginosa* cultures were employed to test the ability of nanoparticles to adsorb toxins in a real environment, and the same efficacy to remove toxins was observed in these conditions. These results suggest the possibility of using the nanotechnology in the treatment of contaminated water or in chemical analysis applications.

Keywords: Phycotoxin, Cyanotoxin, Detoxification, Mitigation, Nanomaterials

1. Introduction

Harmful algal blooms (HABs) are a natural phenomenon that occurs in aquatic ecosystems due to a massive increase in the biomass of certain microorganisms, including dinoflagellate, diatom, or cyanobacteria (Sellner et al. 2003). These blooms have negative impacts to coastal ecosystems and public health. Some of the HABs species produce toxic compounds to humans and animals (Anderson et al. 2015).

Marine toxins, also known as phycotoxins, are produced by phytoplankton (dinoflagellates and diatoms) (Alonso and Alvariño 2018). These toxins can be classified based on their chemical nature in hydrophilic and lipophilic compounds (Botana et al. 2010). The group of hydrophilic toxins includes domoic acid (DA), saxitoxins (STXs) and tetrodotoxins, while the group of lipophilic toxins is composed of, among others, okadaic acid (OA), dinophysistoxins (DTXs), azaspiracids (AZAs), yessotoxins (YTXs) and spirolides (SPXs) (Fig. 1) (Rodriguez et al. 2018). Marine toxins are mainly intracellular, or cell bound; although a portion of toxin can be released into the water (dissolved toxins) (Boerlage and Nada 2015). Both types of toxins, dissolved and intracellular, can be accumulate by seafood like bivalve mollusks which filter large volumes of water to feed on microalgae (Chen et al. 2017, Jauffrais et al. 2013). The consumption of contaminated seafood can cause a wide range of toxic effects in humans including paralytic, neurotoxic, amnesic and diarrheic syndromes (Botana et al. 2010). In order to avoid the consumption of contaminated seafood, regulatory limits and monitoring systems have been developed around the world (Rodríguez et al. 2017).

Massive proliferation of cyanobacteria in freshwater constitutes a potential danger since these organisms produce and release freshwater toxins, also known as cyanotoxins (Fig. 2). According to their toxicity, these compounds can be classified in neurotoxins, hepatotoxins, cytotoxins and dermatoxins. The most relevant freshwater toxins that produce damage in the liver are microcystins (MCs), nodularin (NOD), and cylindrospermopsin (CYN), while anatoxin-a (ATX-a) affects nerve

92 tissue (Merel et al. 2013). Cyanotoxins are mainly intracellular; however, after the cell death these
93 compounds are released to water. As a result, freshwater reservoirs, used as water suppliers, or
94 freshwater aquaculture products can be contaminated (Botana 2016, Roegner et al. 2014).

95 Several control strategies have been developed to eliminate HABs such as mechanical removement
96 of algae, introduction of biological agents that cause algal mortality or chemicals that promote its
97 precipitation (Anderson 2009). The main drawback of these control methods is that the rupture of
98 HAB cells may occur with a subsequent release of intracellular toxins to water. Therefore, treatment
99 processes which include an additional step to remove dissolved toxins are needed (Soltani et al.
100 2017).

101 Different materials have been tested as toxins adsorbents like activated carbon, that can generally
102 adsorb marine and freshwater toxins (Ho and Newcombe 2007, Orr et al. 2004, Pierce et al. 1992),
103 or more selectively, phosphatic clay remove brevotoxins, chitin materials and oyster shells can treat
104 water contaminated with saxitoxin (STX), and molecular imprinted polymers adsorb cyanotoxins
105 (Krupadam et al. 2012, Melegari and Matias 2012, Pierce et al. 2004). However, there are no
106 industrial detoxification protocols which allow the complete elimination of these compounds
107 causing health risks and industrial productivity losses. In the case of marine toxins, harvesting areas
108 need to be closed until blooms disappear and shellfish naturally detoxify (Fosso-Kankeu and Mishra
109 2017, Reboreda et al. 2010). This is a time-consuming process which causes important economic
110 losses in many aquiculture and shellfish related sectors (Reboreda et al. 2010). On the other hand,
111 surface water is usually threated before human consumption; however, conventional drinking water
112 treatment procedures like flocculation, coagulation, sand filtration, membrane filtration or
113 sedimentation are not effective for removing cyanotoxins, which end up, therefore, in the food
114 chain (Fosso-Kankeu and Mishra 2017, Roegner et al. 2014).

115 In the last decades, nanotechnology has become a promising tool for the treatment of water and
116 food contaminated with different compounds. In this regard, several nanoscale and nanostructured

adsorbents have been proposed for the detoxification of contaminated water with a huge variety of compounds such as pesticides, heavy metals or halocarbons (Theron et al. 2008). However, little research has been done to determine the impact of this emerging technology in the elimination of toxins. Nanotechnological applications that have been developed so far include functionalized iron oxide nanoparticles and microparticles to remove microcystin LR (MC-LR) from contaminated water, magnetic covalent organic frameworks to adsorb OA and Dinophysistoxin-1 (DTX1) from seawater, and different types of nanoparticles to adsorb mycotoxins from water solutions and beverages (Gao et al. 2012, González-Jartín et al. 2019, Luo et al. 2017, Magro et al. 2016, Romero et al. 2019).

Therefore, new strategies are needed for the elimination of marine and freshwater toxins from contaminated water. In this context, we have developed a green methodology to remove these compounds from aqueous solutions by using biocompatible nanoparticles that can be magnetically recovered after been used and recycled for several treatments.

2. Materials and methods

2.1. Chemicals and reagents

Acetonitrile (MeCN), methanol (MeOH) and acetic acid (glacial, 100%) were supplied by Panreac Quimica S.A. (Barcelona, Spain). Water was purified in a Millipore Milli-Q Plus system (Millipore, Bedford, MA). Formic acid was from Merck (Madrid, Spain), ammonium formate from Fluka (Buchs, Switzerland), and Durapore centrifugal filters ultrafree-MC (0.22 μm pore size) from Millipore (Billerica, MA). Certified reference materials provided by Laboratorio Cifga S.A. (Lugo, Spain) were: DTX1, Dinophysistoxin-2 (DTX2), OA, Azaspiracid-1 (AZA1), Azaspiracid-2 (AZA2), Azaspiracid-3 (AZA3), 13,19-didesmethyl spirolide C (SPX13,19), 13-desmethyl spirolide C (SPX13), 20-methyl spirolide G (SPX20G), Yessotoxin (YTX), 1a-homoyessotoxin (homoYTX), Saxitoxin dihydrochloride (STX), Decarbamoylsaxitoxin dihydrochloride (dcSTX), Neosaxitoxin dihydrochloride (NEO), Decarbamoylneosaxitoxin dihydrochloride (dcNEO), N-

sulfocarbamoyl gonyautoxin-2&3 (C1, C2), Gonyautoxin-1&3 (GTX1, GTX3), Gonyautoxin-2&4 (GTX2, GTX4), Gonyautoxin-5 (GTX5), Gonyautoxin-6 (GTX6), Decarbamoylgonyautoxin-2&3 (dcGTX2, dcGTX3), ATX-a, NOD, CYN, MC-LR, Microcystin-RR (MC-RR), and desmethyl microcystin MC-LR (dmMC-LR). 3-Aminopropyl(diethoxy)methylsilane (≥ 97%), Tetraethyl orthosilicate (98%), Iron(III) chloride hexahydrate (97%), hydrochloric acid (37%), phosphoric acid (85%), cyclohexane (99.8%), Igepal CO-520 [Polyoxyethylene (5) nonylphenylether, branched], glycerol solution (86-89%), Pluronic® P123[triblock-copolymer-PEO20:PPO70:PEO20,Poly(ethyleneglycol)-block-poly(propyleneglycol)-block-poly(ethyleneglycol)], average Mn ≈ 5800), Rhodamine B isothiocyanate ($C_{29}H_{30}ClN_3O_3S$, RBITC), isooctane (C_8H_{18} ≥99%), 2-propanol (≥99.5%, IPA), Tween® 20 (viscous liquid, polyethylene glycol sorbitan monolaurate), paraformaldehyde (PFA, reagent grade, crystalline) and potassium hexacyanoferrate(II) trihydrate (ACS reagent, 98.5-102.0%) were obtained from Sigma Aldrich; iron(II) sulfate heptahydrate (99%) and ammonium hydroxide (28%) from Fluka Analytical; oleic acid (extra pure) from Merck; ethanol (99.9%) and acetone (≥99%) were purchased at Scharlau. Ferrocene ($Fe(C_5H_5)_2$, ≥98%), hydrogen peroxide (H_2O_2, 30%), and acetone (C_3H_6O, ≥99.9%) were of analytical reagent grade purchased from Aldrich.

2.2. Nanoparticles

In the present work, two different magnetic nanostructured particles, synthesized by wet chemical methods, were developed combining magnetite nanoparticles, Fe_3O_4 NPs, as the magnetic phase, and other inorganic phases (carbon or mesoporous silica) to facilitate chemical affinity with the toxins. Multicore magnetite coated with carbon NPs, m-Fe_3O_4@C, with an average diameter of D=400 nm were prepared by one-step solvothermal process (Vargas-Osorio et al. 2016) while mesoporous silica matrices with Fe_3O_4 NPs anchored over the surface, mesoporous-Si@ Fe_3O_4 , and an average length of L=700 nm, were prepared by a soft template method (Vargas-Osorio et al. 2017). In order to provide a good magnetic response for separation purposes, both nanostructured

materials were designed with a magnetic multicore approach. In addition, to ensure a large number of free sites for toxins' binding, in the case of m-Fe_3O_4@C, all magnetic cores are encapsulated inside, leaving the carbon surface free for adsorption processes, (Fig. 3A) and in the case of mesoporous-Si@ Fe_3O_4, a large extent of the external Si surface, (Fig. 3B) , as well as the free inner channels (with an average diameter around d= 9nm), (Fig. 3C), are available for binding. This morphologically characterization was performed by scanning electron microscopy (SEM) and transmission electron microscopy (TEM), using a Zeiss FE-SEM ULTRA Plus (30 kV) microscope a JEOL JEM-1011 microscope operating at 100 kV, respectively.

The structural characterization was performed by x-ray diffraction (XRD) with a Philips PW1710 diffractometer (Cu Kα radiation source, λ= 1.54186Å). Measurements were collected between $10º<2\theta<80º$ with steps of 0.02º and 5 s/step. The position and relative intensities of the main reflection peaks (Fig. S1) confirms the presence of the magnetite phase in both compounds (JCPDS card No. 19-0629). Textural properties were assessed by performing N_2 adsorption-desorption isotherms using a Quantachrome Autosorb IQ2 instrument. As it can be observed in Fig. S2, all isotherms are type-IV, which is characteristic of mesoporous materials. But, the hysteresis loop is different, in the case of the mesoporous-Si@Fe_3O_4 nanoparticles a H1 loop, typical of materials which exhibit a narrow range of uniform mesopores, is found; meanwhile in the case of m-Fe_3O_4@C a H4 loop, typical of mesoporous carbon, is observed. The surface area is 318.97 and 253.47 cm^3/g for mesoporous-Si@Fe_3O_4 and m-Fe_3O_4@C nanoparticles, respectively. These values are lower than reported from mesoporous SiO_2 and C due to the presence of magnetite. The pore size distribution and specific surface area estimated from the N_2 adsorption-desorption isotherms can be observed in Fig. S2. It can be seen that mesoporous-Si@Fe_3O_4 and m-Fe_3O_4@C nanoparticles present a pore size around 9 and 14 nm, respectively.

Magnetization of all samples was analyzed using a vibrating sample magnetometer (VSM) with an applied field between -10000 and 10000 Oe and working at room temperature. Fig. S3 shows the hysteresis loops of the m-Fe_3O_4@C and mesoporous-Si@ Fe_3O_4 nanoparticles as a function of the

193 applied magnetic field (up to 10 kOe). The materials exhibit a clear superparamagnetic (SPM)
194 behavior and excellent magnetic properties. Also, in the mesoporous-Si@ Fe_3O_4 nanoparticles there
195 is a positive shift in the coercive field, which can be due to magnetostatic interactions in laterally
196 confined structures (Kechrakos and Trohidou 2008).

197 **2.3. Sample solutions and microalgae cultures**

198 Sample solutions were done in Milli-Q water at different concentrations. Standard solution for
199 calibration curves were prepared in HCl 3 mM for hydrophilic toxins, MeOH for lipophilic toxins
200 and Milli-Q water for cyanotoxins.

201 Microalgae cultures were kindly donated by Laboratorio Cifga S.A. Each strain was growing in
202 different and specific media in 500 mL erlenmeyer flasks under controlled conditions.
203 *Gymnodinium catenatum*, was grown in seawater, 33‰ salinity, enriched with L1 medium at 19 ºC.
204 *Prorocentrum lima* was growing in seawater, 30‰ salinity, enriched with TL medium at 24 ºC.
205 *Microcystis aeruginosa* was grown in distillated water enriched with GFWS medium at 19 ºC.

206 **2.4. Chromatography, mass spectrometric conditions and sample treatment**

207 Sample analysis was carried out by using the ultra-performance liquid chromatography - tandem
208 mass spectrometer (UHPLC-MS/MS). A 1290 Infinity UHPLC system coupled to an Agilent
209 G6460C Triple Quadrupole mass spectrometer equipped with an Agilent Jet Stream ESI source was
210 used (Agilent Technologies, Waldbronn, Germany). Samples were held in the autosampler at 4 °C
211 and the injection volume was set at 5µL. The analysis was carried out using multiple reaction
212 monitoring (MRM) acquisition, two product ions were analyzed per compound, one for
213 quantification and the second for confirmation. MassHunter Optimizer software was used to
214 optimize the fragmentor (Frag), cell accelerator voltage (CAV) and collision energy (CE) for each
215 compound. To quantify toxins, lineal 1/X weighted calibration curves were employed, in all cases
216 with correlation coefficients higher to 0.995.

217 **2.4.1 Analysis of hydrophilic toxins**

Aliquots of hydrophilic compounds were acidified before been filtered through 0.22 µm centrifugal filters. Then, toxins were analyzed using a method previously validated (Rodriguez et al. 2018). Briefly, toxins were separated using a column ACQUITY UPLC BEH Amide (2.1x100 mm, 1.7 µm, Waters) at 40 °C. Mobile phase A was 100% water with 0.1% formic acid and 10 mM ammonium formate. Mobile phase B was 98% MeCN containing 0.1% formic acid and 2% 100 mM ammonium formate. Chromatographic separation was performed by using a flow rate of 0.3 mL/min and a gradient of 15 min. The gradient was started at 5%B and raised to 95%B within 11 min. After 1 min at 95%B, the proportion of eluent B was back to 0% in 1 min, and then kept for 2 min for column equilibration. The source conditions were as follows: drying gas temperature 250 ºC, sheath gas temperature 400 ºC, drying gas flow 11 L/min, sheath gas flow 12 L/min, nebulizer gas pressure 55 psi, capillary voltage 3000 V and nozzle voltage 0 V. Transitions and analysis conditions are shown in Table S1.

2.4.2 Analysis of lipophilic toxins

Aliquots of lipophilic toxins were dried using a centrifugal evaporator, reconstituted with 100 µL of MeOH and filtered through 0.22 µm. The method employed for the analysis of lipophilic toxins was previously optimized for the analysis of diarrhetic shellfish poisoning toxins (DSPs), including OA, DTX-1 and DTX-2, in different matrices (Rodriguez et al. 2016, Silva et al. 2015). Transitions for other toxins were optimized by using MassHunter optimizer software. An ACQUITY UPLC BEH C18 (2.1x100 mm, 1.7 µm, Waters) column was employed at 40 °C to separate compounds. Mobile phase A was 100% water and mobile phase B was 95% MeCN and 5% water, both phases containing 50 mM formic acid and 2 mM ammonium formate. Chromatographic separation was performed by using a flow rate of 0.4 mL/min and a gradient of 6.5 min. It was started at 30%B and raised to 70%B within 3 min. Thereafter, the proportion of eluent B was maintained for 1.5 min. Finally, the proportion of eluent B was back to 30% in 0.1 min and maintained for 1.99 min for column equilibration. The source conditions were as follows: drying gas temperature 350 ºC, sheath gas temperature 400 ºC, drying gas flow 8 L/min, sheath gas flow 11 L/min, nebulizer gas pressure

45 psi. In the positive mode, capillary voltage was set at 3500 V and nozzle voltage at 500 V while in the negative mode, capillary voltage was set at 4000 V and nozzle voltage at 0 V. Transitions and analysis conditions are shown in Table S2.

2.4.3 Analysis of freshwater toxins

Aliquots of freshwater toxins were filtered through 0.22 µm centrifugal filters. Then, compounds were separated using a column ACQUITY UPLC HSS T3 column (2.1x100 mm, 1.8 µm, Waters) at 35 °C. Mobile phases were water (A) and MeCN (B), both containing 0.05% formic acid. Chromatographic conditions were previously used for the analysis of cyanotoxins (Rodriguez et al. 2017, Rodriguez et al. 2014). However, small modifications were introduced in the gradient (12 min). After 4 min at 0% of B, the percentage of this eluent was linearly increased to 70% B within 4 min; next, 70% B was maintained for 1 min. Finally, the gradient was switched to 0% B again over 0.5 min, and the column was re-equilibrated for 2.5 min. The flow rate of the mobile phase was kept at 0.3 mL/min. The source conditions were as follows: drying gas temperature 400 ºC, sheath gas temperature 350 ºC, drying gas flow 12 L/min, sheath gas flow 5 L/min, nebulizer gas pressure of 30 psi. The analysis was done in the positive mode using a capillary voltage of 4000 V, and a nozzle voltage of 0 V. The employed transitions and analysis conditions are shown in Table S3. The quantification of toxins for which standards are not available, microcystin AW (MC-AW), microcystin LF (MC-LF), and microcystin LY (MC-LY), was done employing the calibration curve of MC-RR assuming a similar response.

3. Results and Discussion

Eutrophication and climate change might enhance the frequency and magnitude of HABs, and consequently the risk of exposure to naturally occurring toxins (Anderson et al. 2015). Therefore, it is necessary to develop new strategies to deal with these compounds. In this work, we study the use of magnetic nanoparticles as adsorbents for marine and freshwater toxins.

The adsorption capacity of two magnetite based nanostructures combined with different inorganic phases, carbon and mesoporous silica, was first studied. These composites had shown a high efficiency to eliminate mycotoxins (Gonzalez-Jartin et al. 2019). Aqueous solutions were artificially contaminated with a mixture of compounds. The amount of toxins was evaluated before and after treatment by taking aliquots of 100 µL at each time. Aliquots were treated according to the toxin type and subsequently analyzed by UHPLC-MS/MS. All experiments were carried out in triplicate, and controls (solutions without adsorbent addition) were submitted to the same procedure to assess unspecific losses of toxin during the assay. The employed nanoparticles are superparamagnetic, (almost zero coercivity and zero remanence in the magnetization curve) which therefore show enhanced colloidal stability, and their magnetic saturation is high enough to allow for an effective response under the application of moderate magnetic fields. This property ensures a facile separation of the nanoparticles from the liquid matrix by using an external magnet, and it is observed in the experimental procedures that nanoparticles are attracted to the magnet in a few seconds. Commonly we have used a Neodymium Iron Boron (NdFeB) magnet to attract nanoparticles before taking aliquots and, in this way, avoid particle losses.

Initially, carbon and mesoporous silica particles were tested to remove hydrophilic and lipophilic toxins by treating a set of contaminated aqueous solutions with 250 µg of nanoparticles (125 mg/L) for 60 min. The amount of toxin eliminated by each type of particle is shown in Fig. S4. Carbon nanoparticles attained reductions near to 45% applied to hydrophilic toxins, STX, dcSTX and NEO, and reductions about 90% for lipophilic toxins AZAs and SPX20G. Silica particles were no effective removing hydrophilic toxins and AZAs. OA, DTX1 and SPX20G were adsorbed in silica particles in a lower proportion, while YTX was removed in a higher proportion, 43%. Therefore, carbon nanoparticles were selected to further study the ability to adsorb each group of toxins.

First, hydrophilic toxins were checked. This group of toxins can be divided, according to the charge of their molecules, in three groups (Fig. 1), C toxins (charge 0), GTXs (charge 1), and STXs (charge 2). In the previous experiments, a solution with 11 toxins was used. Therefore, the adsorption of

each group was studied independently to avoid competition for sorption sites. In addition, to check the saturation capacity, two amounts of nanostructures were used, 250 and 500 µg (equivalently 125 and 250 mg/L), in the presence of 20 µg/L of each toxin. Fig. 4 shows the percentage of removed toxins and the adsorption capacity, expressed as µg/g, for each compound after 60 min of incubation with nanoparticles. The detoxification capacity for C1 toxin was low, since only 6.21% of toxin was removed (Fig. 4A). In the case of GTXs, when 500 µg of nanoparticles were used, toxin reductions varied from 5% for dcGTX3 to 13% for GTX3 (Fig. 4A). With regard to STXs (STX, NEO, dcSTX, dcNEO), the use of 500 µg of nanoparticles yielded toxin reductions between 58% for dcNEO and 72% for STX (Fig. 4A). The reduction in the number of particles by half caused a proportional decrease in the percentage of eliminated toxin. For instance, the adsorption of STX decreased from 72% to 44% when the number of composites was reduced from 500 to 250 µg. Reductions were similar to those obtained when 250 µg were used to treat a mixture of hydrophilic toxins (Cs, GTXs and STXs) (Fig. S4), indicating that these compounds do no compete for sorption sites. When the adsorption was evaluated as µg of toxin adsorbed by gram of nanoparticles, similar data was obtained with 500 µg and 250 µg (Fig. 4B). In the case of STX, the adsorption reached with 500 µg of particles was 45 µg/g and with 250 µg of particles was 61 µg/g. Therefore, for STXs (STX, dcSTX, NEO, dcNEO) the maximum adsorption is around 200 µg/g. The use of oyster shells and chitin materials as STX adsorbents was previously proposed (Melegari and Matias 2012). The adsorption capacity of the present nanoparticles is much larger than those reported materials. In addition, the time of treatment using these magnetic nanocomposites is strongly reduced from several hours to 60 min. Hydrophilic marine toxins included in this study belong to the group of paralytic shellfish poisoning (PSP) toxins. These compounds have a common structure characterized by containing guanidino groups as their main components, which are responsible for their high polarity (Suarez-Isla 2016). Each toxin of these group has different functional side groups (Fig. 1), that could explain different affinity for nanoparticles. Specifically, C1 and GTXs, with sulfate side groups in their structure show a poor adsorption to the carbon coated nanostructures. As

it has been previously reported, molecules with sulfate groups are weakly adsorbed by activated carbon (Duman and Ayranci 2006). In this sense, at the pH of the Milli-Q water (6.99) in which the experiment was carried out, the surface charge of the activated carbon is negative due to the presence of negatively charged carboxylate and anhydride anionic surface functional groups (Huang et al. 2007, Riché et al. 2006). The carboxylic acid moieties of activated carbon can form electrostatic interactions with the amine moieties of charge 2 hydrophilic toxins (STXs). The simultaneous presence of repulsive (from the sulfate) and attractive (from the amine) forces in C toxins (charge 0), GTXs (charge 1) might reduce the interaction (Culver et al. 2017, Olano et al. 2020). Therefore, the sulfate functional groups of these toxins can be responsible for their fair adsorption of the nanostructure surface.

Next, the removal of lipophilic toxins was studied. The initial experiment that was carried out using aqueous solution contaminated with seven toxins at 10 µg/L. Therefore, as in the case of hydrophilic toxins, the adsorption of each group was now studied according to their structure in four groups: OA, DTX1 and DTX2 as DSPs, the group of AZAs included AZA1, AZA2 and AZA3, YTX and homoYTX composed the group of YTXs, and the group of SPXs was formed by SPX13, SPX13,19, and SPX20G. In all cases, solutions were contaminated with 20 µg/L and treated with 500 and 250 µg of carbon nanoparticles. The incubation of 500 µg of composites with DSPs removed near to 40% of these compounds, while 250 µg of composites adsorbed around the 15%, with a maximum adsorption of 47 µg of DSPs per gram of nanoparticles (Fig. 5A,B). In the case of AZAs, similar reductions were obtained with both amounts of nanoparticles. For instance, in the case of AZA1, 500 µg of composites removed 72% while a reduction of 59% was reached with 250 µg (Fig. 5A). Consequently, the adsorption capacity was doubled, from 127 µg/g of AZAs (AZA1, AZA2 and AZA3) to 242 µg/g when the amount of particles was halved (Fig. 5B). Therefore, nanoparticles were not saturated and the maximum adsorption for these toxins is much greater. Next, the elimination of YTXs was studied. In this case, reductions lower to 15% were obtained when 500 µg of nanoparticles where used, while with 250 µg this percentage decrease to 8.5% (Fig.

346 5A). With regard to the adsorption, similar data were obtained with the two amounts of tested
347 adsorbent, with a maximum uptake of 8.36 µg/g for YTX and 5.91 for homoYTX (Fig. 5B).
348 Finally, the adsorption of SPXs was evaluated. The use of 500 and 250 µg of nanoparticles yielded
349 similar reduction percentages (Fig. 5A). SPX20G was eliminated in a greater proportion with
350 reductions of 72.8% when 500 µg were used, and 71.1% when the amount of adsorbent was 250 µg.
351 In the case of the SPX13,19 and SPX13, near to 53% was eliminated with 500 µg, while with 250
352 µg this percentage was 43% (Fig. 5A). The adsorption of these compounds was increased when the
353 number of nanoparticles decreased from 500 to 250 µg. For instance, the adoption capacity for
354 SPX20G was raised from 41.65 to 93.63 µg/g when the amount of particles was halved (Fig. 5B).
355 Hence, an adsorption of 210 µg/g was reached for SPXs by using 250 µg of nanoparticles.
356 However, as in the case of AZAs, composites were not saturated since similar adsorption
357 percentages were obtained with 500 and 250 µg of nanoparticles, and therefore the maximum
358 adsorption could be much greater. Compounds included in the groups of lipophilic toxins have
359 different structures (Fig. 1), and therefore the ability of nanoparticles to eliminate them depends on
360 the toxin group. In this sense, SPXs and AZAs were highly removed, around a 70%, DSPs were
361 also eliminated although in a smaller proportion, while only small amounts of YTXs were adsorbed.
362 YTXs are polyether compounds containing two sulfate groups, which made these toxins the most
363 polar within the group of the lipophilic toxins (Paz et al. 2008). Therefore, as in the case of the
364 hydrophilic compounds, the presence of sulfate groups may avoid their adsorption by nanoparticles.

365 Since either hydrophilic and lipophilic toxins are highly eliminated with 250 µg of carbon
366 nanocomposites, next, the ability to eliminate freshwater toxins was tested. In these experiments, a
367 mixture of ATX-a, NOD, CYN, MC-LR, and MC-RR was treated with 250 µg of carbon
368 nanoparticles for 60 min. As Fig. 6A shows, 84.72% of MC-RR, 62.21% of MC-LR and 31.09% of
369 NOD were removed, while reductions lower to 10% were obtained for ATX-a and CYN. The
370 adsorption capacity for each toxin expressed as µg/g is shown in Fig. 6B. Each gram of
371 nanoparticles can remove up to 376.72 µg of freshwater toxins as follows: 168.70 µg of MC-LR,

372 99.37 of µg MC-RR, 69.41 of µg NOD, 32.40 of CYN and 6.8 µg of ATX-a (Fig. 6B). The
373 adsorption capacity for MC-LR slightly improves the elimination previously achieved by using iron
374 oxide nanoparticles (Gao et al. 2012). The World Health Organization has recommended a
375 maximum of 1µg/L for MC-LR in drinking water (WHO 2017). Therefore, 1 g of nanoparticles
376 could be used to treat 168 L of water contaminated with 1µg/L of MC-LR, and this process would
377 reduce the contamination to 0.37 µg/L, making it safer for human consumption. The adsorption of
378 freshwater toxins depends on their structure (Fig. 2) and the chemical surface of the adsorbent,
379 giving rise to a high variability in the efficiency of the removement process: cyclic peptides, MCs
380 and NOD, where highly removed by carbon nanoparticles, while only low amounts of the alkaloids
381 ATX-a and CYN were eliminated from solutions.

382 The kinetics of the adsorption of marine toxins were tested by taking aliquots of 100 µL at 5, 10,
383 15, 30, and 60 min. The percentage of toxin removed by 250 µg of nanoparticles at each time for
384 those compounds with adsorptions higher to 15% is shown in Fig. S5. In general, the maximum
385 elimination was reached at 5 min, and then the percentage of removed toxin remained constant (Fig.
386 S5A-C). However, there were an increasing trend in the amount of SPXs eliminated as function of
387 time (Fig. S5D). For instance, although 23.07% of SPX13,19 was eliminated after 5 min of
388 incubation, this percentage continued to increase to 31.45% after 30 min and it reached 42.96%
389 after 60 min. The kinetics of adsorption of freshwater toxins was tested by taking aliquots of 100
390 µL at 15, 30, and 60 min. The percentage of toxin eliminated at each time is shown in Fig. S5E,
391 showing a time dependent adsorption curve, that steadily increased up to the maximum attained
392 after 60 min of contact time. This time-dependent sorption behavior observed for SPXs and
393 freshwater toxins can be ascribed to a process in which saturation of adsorbent surface first
394 happens and is then followed by a slow adsorption inside inner pores (Santhi et al. 2016).

395 Next, the feasibility of toxin recovery from the nanoparticles surface was determined by immersing
396 them into a designed solvent mixture depending on the toxin nature. Solutions were vortexed for 5
397 min and then sonicated, 5 min 50/60 Hz. In the case of hydrophilic toxins, the solvent was HCl 3

mM, MeOH in the case of lipophilic toxins, and MeOH 75% was used to detach freshwater toxins. Afterwards, nanoparticles were removed from solutions using the NdFeB magnet and the supernatant was subsequently filtered through 0.22 µm. The amount of toxin in the extract was measured by UHPLC-MS/MS and the percentage of recovered toxin was calculated (Fig. S6). In this sense, near to 80% of hydrophilic toxins were detached (Fig. S6A). In general, a complete recovery was achieved for lipophilic toxins (Fig. S6B). However, in the case of OA, around 40% of this toxin was recovered with the extraction procedure. Finally, the desorption rate for freshwater toxins varied from 90% of MC-LR to 14% of CYN, while an intermediate recovery, around 50%, was obtained for MC-RR and NOD (Fig. S6C). Freshwater toxins were extracted with MeOH 75% (Ramanan et al. 2000). With these solvent MC-LR was almost completely recovered. Adsorbents should allow a simple and fast desorption in order to be employ at the industrial level (Ali et al. 2017). In this sense, a satisfactory recovery was achieved for marine toxins and some freshwater toxins, which would allow the recycling and reuse of the composites.

Finally, in order to evaluate the effectivity of the nanoparticles in a real environment, cultures of *Gymnodinium catenatum*, *Prorocentrum lima*, and *Microcystis aeruginosa* were employed. In this sense, *G. catenatum* and *P. lima* samples contained 3400 cells/mL and 216 cells/mL, respectively, while *M. aeruginosa* culture contained 1.62 x 10^6 cells/mL. All cultures were sonicated prior to use, 10 cycles of 1 min at 40% intensity (Sonopuls HD 4050; Bandelin), to break the cells and thus increase the release of toxin to the water. First, the toxigenic profile of each specie was studied. In this sense, *G. catenatum* produced high amounts of C1 and C2 toxins, 3876 and 266 µg/L respectively, as well as dcSTX (45 µg/L), dcNEO (39 µg/L), GTX3 (312 µg/L), GTX5 (255 µg/L), and GTX6 (113 µg/L). This culture was spiked with 20 µL/L of STX. The *P. lima* culture contained OA (33 µg/L) and DTX1 (17 µg/L), and *M. aeruginosa* produced MC-LR (158 µg/L), dmMC-LR (77 µg/L), MC-RR (11 µg/L), and low amounts, inferior to 2 µg/L, of MC-AW, MC-LF and MC-LY. Next, 2 mL of each culture were treated with 250 µg of carbon nanoparticles (125 mg/L) for 60 min. Results are shown in Fig.7. The treatment of *G. catenatum* culture yielded toxin reductions for

STX, dcSTX and dcNEO, while, as expected, the concentration of C and GTXs was not significantly reduced. Toxin adsorption from the culture was similar to that reached in aqueous solution. For example, there was the same concentration of STX in both matrices and a similar reduction was obtained, 43.77% in aqueous solutions (Fig. 4A) and 44.46% in cultures (Fig. 7A). The adsorption capacity for STXs (sum of: STX, dcSTX, NEO and dcNEO) in aqueous solutions was 223.80 µg/g (Fig. 4B), while from cultures each gram of nanoparticles adsorbed 265.71 µg of the sum of STXs (Fig. 7B). Therefore, the adsorption capacity for hydrophilic toxins was maintained. The *P. lima* culture contained 32.55 µg/L of OA and 16.45 µg/L of DTX1, the treatment of the culture yielded reductions of 12.72% and 10.05%, respectively (Fig. 7A). Again, reductions were similar to those observed in aqueous solutions (Fig. 5A). Nanoparticles uptake 41.95 µg/g of DSPs (OA, DTX1 and DTX2) from aqueous solutions (Fig. 5B), and 46.6 µg/g (OA, and DTX1) from *P. lima* culture (Fig. 7B). Consequently, the adsorption for lipophilic toxins was also maintained in a real environment. Finally, the *M. aeruginosa* culture was treated with nanoparticles. In these conditions, reductions of 26.51% of MC-RR, 43.29% of MC-LR and 27.13% dmMC-LR were obtained (Fig. 7A). The percentage of removed toxin from cultures is lower than the elimination reached from aqueous solutions. For instance, 46% of MC-LR was removed from cultures while the removal of this toxin from aqueous solutions reached the 62.21%. This lower percentage of reduction is due to the high amount of MC-LR in the culture (158 µg/L), while the aqueous solutions contained 50 µg/L of this toxin. However, the higher amount of microcystins in the culture yielded an adsorption of 729.89 µg/g, while in aqueous solutions the amount of adsorbed compounds was 376.72 µg/g. Hence, the elimination of cyanotoxins from contaminated water was also maintained in *M. aeruginosa* culture. Culture solutions contained broken microalgae cells, trace metal and vitamins from the enrichment medium. In addition, marine toxin solutions contained salt at concentrations levels of the real environment. The presence of salt and organic matter may strongly affect the adsorption. However, the adsorption of carbon nanoparticles was maintained even with the high amounts of broken cells and salts in solutions, and the adsorption

capacity is in the range of other previously studied materials (Table S4). Therefore, these results show the high efficacy of the nanoparticles to adsorb marine toxins and cyanotoxins in a real environment.

Nanoparticles show to be versatile in removing a wide set of dissolved toxins, that are of concern for human health, with high percentages of adsorption, efficient magnetic separation and the additional advantage of reusability, since marine and freshwater toxins can be easily recovered from nanoparticles. Therefore, nanotechnology offers new and effective approaches for water treatment processes in which additional cleaning barriers are highly required to remove toxins. For instance, depuration (purification) is a procedure by which shellfish are placed in tanks of clean seawater for several hours or days, and during this period, contaminants, mainly microbial, are eliminated from their gills and intestinal tract (Lee et al. 2008). However, the elimination of marine toxins is a slow process, and the compounds which are expelled during depuration can enter again into the shellfish under treatment (Svensson 2003). Therefore, nanoparticles could be used as a preventive measure, to eliminate excreted marine toxins from water and to avoid further recontamination. This application could be of a special interest in those plants using recirculating systems in which seawater is reused from one depuration cycle to another (Lee et al. 2008). Other possible applications include the monitoring of toxin profile in seawater and the samples analysis in the laboratory. Solid Phase Adsorption Toxin Tracking (SPATT) is a passive methodology that allows the detection of dissolved toxins in water as an alert system. This technique involves the immersion of small bags containing an adsorbent in the water body, that after a period of time are recovered (Rodríguez et al. 2011). Afterwards, adsorbed toxins are extracted and quantified, allowing to determine which toxins are released during algal blooms (Mashile and Nomngongo 2017). On the other hand, the most common extraction procedures for the analysis of marine toxins include clean up steps; mainly, solid-phase extraction (SPE), in which however the matrix effect cannot be eliminated. A possible solution to cancel the interference of compounds from matrix could be the use of different nanoparticles to trap the extracted toxins. This procedure, known as magnetic solid-

phase extraction (MSPE), has been recently proposed for sampling , preconcentrating and cleaning up, and it has been successfully applied to the analysis of DA marine toxin (Zhang et al. 2015). Therefore, as shown in precedent sections, nanocomposites have an important adsorption capacity, can be further recovered by extraction with different solvents for which we propose them as valuable tools for detoxification systems, for SPATT and MSPE applications or in the treatment of drinking water.

4. Conclusion

Magnetic carbon core-shell nanoparticles are highly effective to remove marine and freshwater toxins. The adsorption capacity is related with their structure and the chemical nature of the adsorbents. When carbon coated magnetic nanostructures are used, around 70% of marine toxins that do not have sulfate groups in their structure and up to 84.7% freshwater toxins with cyclic peptide structures can be eliminated from solutions. The adsorption capacity is maintained in natural enviroment. Magnetic separation, which has an efficient performance with multicore magnetite based nanostructures, is a cheap and green technology that allows for the total recovery of the adsorbent materials. Moreover, toxins can be recovered from composites which would allow and additional use as reusable nanoplatforms for chemical analysis.

Acknowledgments

The research leading to these results has received funding from the following FEDER cofunded-grants. From Conselleria de Cultura, Educacion e Ordenación Universitaria, Xunta de Galicia, 2017 GRC GI-1682 (ED431C 2017/01) and the Strategic Grouping in Materials (AEMAT)/Grant No. ED431E2018/08. From CDTI and Technological Funds, supported by Ministerio de Economía, Industria y Competitividad, AGL2016-78728-R (AEI/FEDER, UE), ISCIII/PI16/01830 and RTC-2016-5507-2, ITC-20161072. From European Union POCTEP 0161-Nanoeaters -1-E-1, Interreg AlertoxNet EAPA-317-2016, Interreg Agritox EAPA-998-2018, and H2020 778069-EMERTOX.

Jesús M. González-Jartín was supported by a fellowship from Programa de Formación de Profesorado Universitario (FPU14/00166), Ministerio de Educación, Cultura y Deporte, Spain.

Appendix A. Supplementary data

References:

Ali, I., Alothman, Z.A. and Alwarthan, A., 2017. Uptake of propranolol on ionic liquid iron nanocomposite adsorbent: Kinetic, thermodynamics and mechanism of adsorption. J. Mol. Liq. 236, 205-213.

Alonso, E. and Alvariño, R., 2018. Marine Toxins, in: Botana, L.M. (Ed.), Envirometal Toxicology. De Gruyter, Berlin, pp. 147-167.

Anderson, C.R., Moore, S.K., Tomlinson, M.C., Silke, J. and Cusack, C.K., 2015. Living with harmful algal blooms in a changing world: strategies for modeling and mitigating their effects in coastal marine ecosystems, in: Ellis, J. T., Sherman, D. J. (Eds.), Coastal and Marine Hazards, Risks, and Disasters. Elsevier, Amsterdam, pp. 495-561.

Anderson, D.M., 2009. Approaches to monitoring, control and management of harmful algal blooms (HABs). Ocean Coast. Manag. 52(7), 342-347.

Boerlage, S. and Nada, N., 2015. Algal toxin removal in seawater desalination processes. Desalin. Water Treat. 55(10), 2575-2593.

Botana, L.M., 2016. Toxicological Perspective on Climate Change: Aquatic Toxins. Chem. Res. Toxicol. 29(4), 619-625.

Botana, L.M., Vilariño, N., Alfonso, A., Vale, C., Louzao, C., Elliott, C.T., Campbell, K. and Botana, A.M., 2010. The problem of toxicity equivalent factors in developing alternative methods to animal bioassays for marine-toxin detection. TrAC, Trends Anal. Chem. 29(11), 1316-1325.

Chen, J., Li, X., Wang, S., Chen, F., Cao, W., Sun, C., Zheng, L. and Wang, X., 2017. Screening of lipophilic marine toxins in marine aquaculture environment using liquid chromatography–mass spectrometry. Chemosphere 168, 32-40.

Culver, H.R., Sharma, I., Wechsler, M.E., Anslyn, E.V. and Peppas, N.A., 2017. Charged poly(N-isopropylacrylamide) nanogels for use as differential protein receptors in a turbidimetric sensor array. Analyst 142(17), 3183-3193.

Duman, O. and Ayranci, E., 2006. Adsorption Characteristics of Benzaldehyde, Sulphanilic acid, and p- Phenolsulfonate from Water, Acid, or Base Solutions onto Activated Carbon Cloth. Sep. Sci. Technol. 41(16), 3673-3692.

Fosso-Kankeu, E. and Mishra, A.K., 2017. 9 - Photocatalytic degradation and adsorption techniques involving nanomaterials for biotoxins removal from drinking water, in: Grumezescu, A.M. (Ed.), Water Purification. Academic Press, London, pp. 323-354.

Gao, Y.Q., Gao, N.Y., Deng, Y., Gu, J.S., Shen, Y.C. and Wang, S.X., 2012. Adsorption of microcystin-LR from water with iron oxide nanoparticles. Water Environ. Res. 84(7), 562-568.

Gonzalez-Jartin, J.M., de Castro Alves, L., Alfonso, A., Pineiro, Y., Vilar, S.Y., Gomez, M.G., Osorio, Z.V., Sainz, M.J., Vieytes, M.R., Rivas, J. and Botana, L.M., 2019. Detoxification agents based on magnetic nanostructured particles as a novel strategy for mycotoxin mitigation in food. Food Chem. 294, 60-66.

González-Jartín, J.M., de Castro Alves, L., Alfonso, A., Piñeiro, Y., Vilar, S.Y., Gomez, M.G., Osorio, Z.V., Sainz, M.J., Vieytes, M.R., Rivas, J. and Botana, L.M., 2019. Detoxification agents based on magnetic nanostructured particles as a novel strategy for mycotoxin mitigation in food. Food Chem. 294, 60-66.

Ho, L. and Newcombe, G., 2007. Evaluating the adsorption of microcystin toxins using granular activated carbon (GAC). J. Water Supply: Res. Technol. - AQUA 56(5), 281-291.

Huang, W.J., Cheng, B.L. and Cheng, Y.L., 2007. Adsorption of microcystin-LR by three types of activated carbon. J. Hazard. Mater. 141(1), 115-122.

549 Jauffrais, T., Kilcoyne, J., Herrenknecht, C., Truquet, P., Sechet, V., Miles, C.O. and Hess, P.,
550 2013. Dissolved azaspiracids are absorbed and metabolized by blue mussels (*Mytilus edulis*).
551 Toxicon 65, 81-89.
552 Kechrakos, D. and Trohidou, K.N., 2008. Dipolar interaction effects in the magnetic and
553 magnetotransport properties of ordered nanoparticle arrays. J. Nanosci. Nanotechnol. 8(6), 2929-
554 2943.
555 Krupadam, R.J., Patel, G.P. and Balasubramanian, R., 2012. Removal of cyanotoxins from surface
556 water resources using reusable molecularly imprinted polymer adsorbents. Environ. Sci. Pollut. Res.
557 Int. 19(5), 1841-1851.
558 Lee, R., Lovatelli, A. and Ababouch, L., 2008. Bivalve depuration: fundamental and practical
559 aspects. FAO Fisheries Technical Paper. No. 511, Rome.
560 Luo, Y., Zhou, Z. and Yue, T., 2017. Synthesis and characterization of nontoxic chitosan-coated
561 Fe3O4 particles for patulin adsorption in a juice-pH simulation aqueous. Food Chem. 221, 317-323.
562 Magro, M., Moritz, D.E., Bonaiuto, E., Baratella, D., Terzo, M., Jakubec, P., Malina, O., Cepe, K.,
563 Aragao, G.M.F., Zboril, R. and Vianello, F., 2016. Citrinin mycotoxin recognition and removal by
564 naked magnetic nanoparticles. Food Chem. 203, 505-512.
565 Mashile, G.P. and Nomngongo, P.N., 2017. Recent Application of Solid Phase Based Techniques
566 for Extraction and Preconcentration of Cyanotoxins in Environmental Matrices. Crit. Rev. Anal.
567 Chem. 47(2), 119-126.
568 Melegari, S.P. and Matias, W.G., 2012. Preliminary assessment of the performance of oyster shells
569 and chitin materials as adsorbents in the removal of saxitoxin in aqueous solutions. Chem. Cent. J.
570 6(1), 86.
571 Merel, S., Walker, D., Chicana, R., Snyder, S., Baures, E. and Thomas, O., 2013. State of
572 knowledge and concerns on cyanobacterial blooms and cyanotoxins. Environ. Int. 59, 303-327.

573 Olano, D.E.B., Salvador-Reyes, L.A., Montaño, M.N.E. and Azanza, R.V., 2020. Sorption of
574 paralytic shellfish toxins (PSTs) in algal polysaccharide gels. Algal Res. 45, 101655.
575 http://dx.10.1016/j.algal.2019.101655.
576 Orr, P.T., Jones, G.J. and Hamilton, G.R., 2004. Removal of saxitoxins from drinking water by
577 granular activated carbon, ozone and hydrogen peroxide-implications for compliance with the
578 Australian drinking water guidelines. Water Res. 38(20), 4455-4461.
579 Paz, B., Daranas, A.H., Norte, M., Riobo, P., Franco, J.M. and Fernandez, J.J., 2008. Yessotoxins, a
580 group of marine polyether toxins: an overview. Mar. Drugs 6(2), 73-102.
581 Pierce, R.H., Henry, M.S., Higham, C.J., Blum, P., Sengco, M.R. and Anderson, D.M., 2004.
582 Removal of harmful algal cells (*Karenia brevis*) and toxins from seawater culture by clay
583 flocculation. Harmful Algae 3(2), 141-148.
584 Pierce, R.H., Henry, M.S., Proffitt, L.S. and deRosset, A.J., 1992. Evaluation of solid sorbents for
585 the recovery of polyether toxins (brevetoxins) in seawater. Bull. Environ. Contam. Toxicol. 49(4),
586 479-484.
587 Ramanan, S., Tang, J. and Velayudhan, A., 2000. Isolation and preparative purification of
588 microcystin variants. J. Chromatogr. A 883(1-2), 103-112.
589 Reboreda, A., Lago, J., Chapela, M.-J., Vieites, J.M., Botana, L.M., Alfonso, A. and Cabado, A.G.,
590 2010. Decrease of marine toxin content in bivalves by industrial processes. Toxicon 55(2), 235-243.
591 Riché, E., Carrié, A., Andin, N. and Mabic, S., 2006. High-purity water and pH. Am. Lab. 38(13),
592 22.
593 Rodriguez, I., Alfonso, A., Antelo, A., Alvarez, M. and Botana, L.M., 2016. Evaluation of the
594 Impact of Mild Steaming and Heat Treatment on the Concentration of Okadaic Acid,
595 Dinophysistoxin-2 and Dinophysistoxin-3 in Mussels. Toxins 8(6), 175-187.
596 Rodriguez, I., Alfonso, A., Gonzalez-Jartin, J.M., Vieytes, M.R. and Botana, L.M., 2018. A single
597 run UPLC-MS/MS method for detection of all EU-regulated marine toxins. Talanta 189, 622-628.

598 Rodriguez, I., Fraga, M., Alfonso, A., Guillebault, D., Medlin, L., Baudart, J., Jacob, P., Helmi, K.,
599 Meyer, T., Breitenbach, U., Holden, N.M., Boots, B., Spurio, R., Cimarelli, L., Mancini, L.,
600 Marcheggiani, S., Albay, M., Akcaalan, R., Koker, L. and Botana, L.M., 2017. Monitoring of
601 freshwater toxins in European environmental waters by using novel multi-detection methods.
602 Environ. Toxicol. Chem. 36(3), 645-654.
603 Rodriguez, I., Rodriguez, C., Alfonso, A., Otero, P., Meyer, T., Breitenbach, U. and Botana, L.M.,
604 2014. Toxin profile in samples collected in fresh and brackish water in Germany. Toxicon 91, 35-
605 44.
606 Rodríguez, I., Vieytes, M.R. and Alfonso, A., 2017. Analytical challenges for regulated marine
607 toxins. Detection methods. Curr. Opin. Food Sci. 18, 29-36.
608 Rodríguez, P., Alfonso, A., Turrell, E., Lacaze, J.-P. and Botana, L.M., 2011. Study of solid phase
609 adsorption of paralytic shellfish poisoning toxins (PSP) onto different resins. Harmful Algae 10(5),
610 447-455.
611 Roegner, A.F., Brena, B., Gonzalez-Sapienza, G. and Puschner, B., 2014. Microcystins in potable
612 surface waters: toxic effects and removal strategies. J. Appl. Toxicol. 34(5), 441-457.
613 Romero, V., Fernandes, S.P.S., Rodriguez-Lorenzo, L., Kolen'ko, Y.V., Espina, B. and Salonen,
614 L.M., 2019. Recyclable magnetic covalent organic framework for the extraction of marine
615 biotoxins. Nanoscale 11(13), 6072-6079.
616 Santhi, T., Manonmani, S., Vasantha, V.S. and Chang, Y.T., 2016. A new alternative adsorbent for
617 the removal of cationic dyes from aqueous solution. Arabian J. Chem. 9, S466-S474.
618 Sellner, K.G., Doucette, G.J. and Kirkpatrick, G.J., 2003. Harmful algal blooms: causes, impacts
619 and detection. J. Ind. Microbiol. Biotechnol. 30(7), 383-406.
620 Silva, M., Rodriguez, I., Barreiro, A., Kaufmann, M., Isabel Neto, A., Hassouani, M., Sabour, B.,
621 Alfonso, A., Botana, L.M. and Vasconcelos, V., 2015. New Invertebrate Vectors of Okadaic Acid
622 from the North Atlantic Waters-Portugal (Azores and Madeira) and Morocco. Toxins 7(12), 5337-
623 5347.

624 Soltani, A., Hess, P., Dixon, M.B., Boerlage, S.F.E., Anderson, D.M., Newcombe, G., House, J.,
625 Ho, L., Baker, P. and Burch, M., 2017. World Health Organization and international guidelines for
626 toxin control, harmful algal bloom management, and response planning. Intergovernmental
627 Oceanographic Commission. http://dx.doi.org/10.25607/OBP-313
628 Suarez-Isla, B.A., 2016. Saxitoxin and Other Paralytic Toxins: Toxicological Profile, in:
629 Gopalakrishnakone, P., Haddad Jr, V., Tubaro, A., Kim, E. and Kem, W.R. (Eds.), Marine and
630 Freshwater Toxins. Springer, Netherlands, pp. 23-41.
631 Svensson, S., 2003. Depuration of Okadaic acid (Diarrhetic Shellfish Toxin) in mussels, *Mytilus*
632 *edulis* (*Linnaeus*), feeding on different quantities of nontoxic algae. Aquaculture 218(1), 277-291.
633 Theron, J., Walker, J.A. and Cloete, T.E., 2008. Nanotechnology and water treatment: applications
634 and emerging opportunities. Crit. Rev. Microbiol. 34(1), 43-69.
635 Vargas-Osorio, Z., Argibay, B., Piñeiro, Y., Vázquez-Vázquez, C., López-Quintela, M.A., Álvarez-
636 Pérez, M.A., Sobrino, T., Campos, F., Castillo, J. and Rivas, J., 2016. Multicore Magnetic
637 Fe3O4@C Beads With Enhanced Magnetic Response for MRI in Brain Biomedical Applications.
638 IEEE Trans. Magn. 52(7), 1-4.
639 Vargas-Osorio, Z., González-Gómez, M.A., Piñeiro, Y., Vázquez-Vázquez, C., Rodríguez-Abreu,
640 C., López-Quintela, M.A. and Rivas, J., 2017. Novel synthetic routes of large-pore magnetic
641 mesoporous nanocomposites (SBA-15/Fe3O4) as potential multifunctional theranostic nanodevices.
642 J. Mater. Chem. B 5(47), 9395-9404.
643 WHO, 2017. Guideline values for chemicals that are of health significance in drinking-water,
644 Guidelines for Drinking-Water Quality: Fourth Edition Incorporating the First Addendum, Geneva.
645 Zhang, W., Yan, Z., Gao, J., Tong, P., Liu, W. and Zhang, L., 2015. Metal-organic framework UiO-
646 66 modified magnetite@silica core-shell magnetic microspheres for magnetic solid-phase extraction
647 of domoic acid from shellfish samples. J. Chromatogr. A 1400, 10-18.

Figure 1

Click here to download Figure: Figure 1.pptx

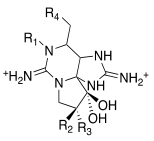

PSPs

Toxin	R1	R2	R3	R4
C1	H	H	OSO_3^-	$OCONHSO_3^-$
C2	H	OSO_3^-	H	$OCONHSO_3^-$
GTX5	H	H	$OCONHSO_3^-$	
GTX6	OH	H	H	$OCONHSO_3^-$
dcGTX2	H	H	OSO_3^-	OH
dcGTX3	H	OSO_3^-	H	OH
dcSTX	H	H	H	OH
dcNEO	OH	H	H	OH
GTX2	H	H	OSO_3^-	$OCONH_2$
GTX3	H	OSO_3^-	H	$OCONH_2$
GTX1	OH	H	OSO_3^-	$OCONH_2$
GTX4	OH	OSO_3^-	H	$OCONH_2$
STX	H	H	H	$OCONH_2$
NEO	OH	H	H	$OCONH_2$

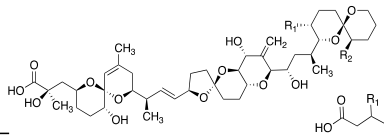

DSPs

Toxin	R1	R2
OA	CH_3	H
DTX1	CH_3	CH_3
DTX2	H	CH_3

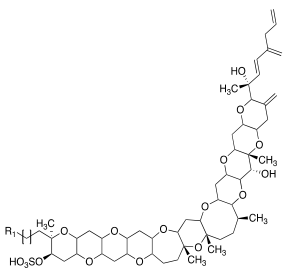

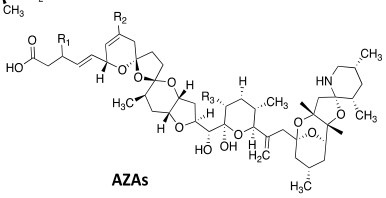

AZAs

Toxin	R1	R2	R3
AZA1	H	H	CH_3
AZA2	H	CH_3	CH_3
AZA3	H	H	H

YTXs

Toxin	n	R1
YTX	1	OSO_3Na
Homo-YTX	2	OSO_3Na

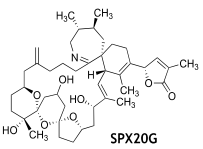

SPX20G

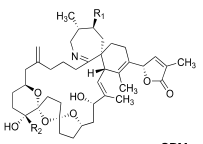

SPXs

Toxin	R1	R2
SPX13	CH_3	CH_3
SPX13,19	CH_3	H

Figure 2

Click here to download Figure: Figure 2.pptx

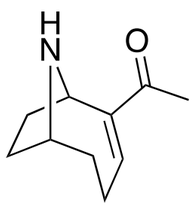

ATX-a

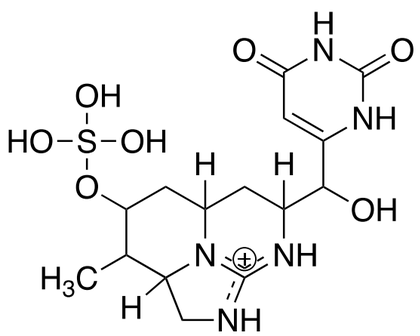

CYN

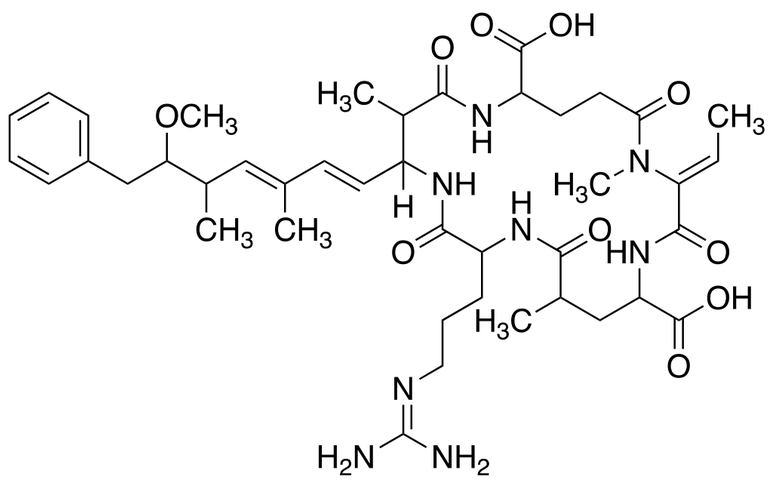

NOD

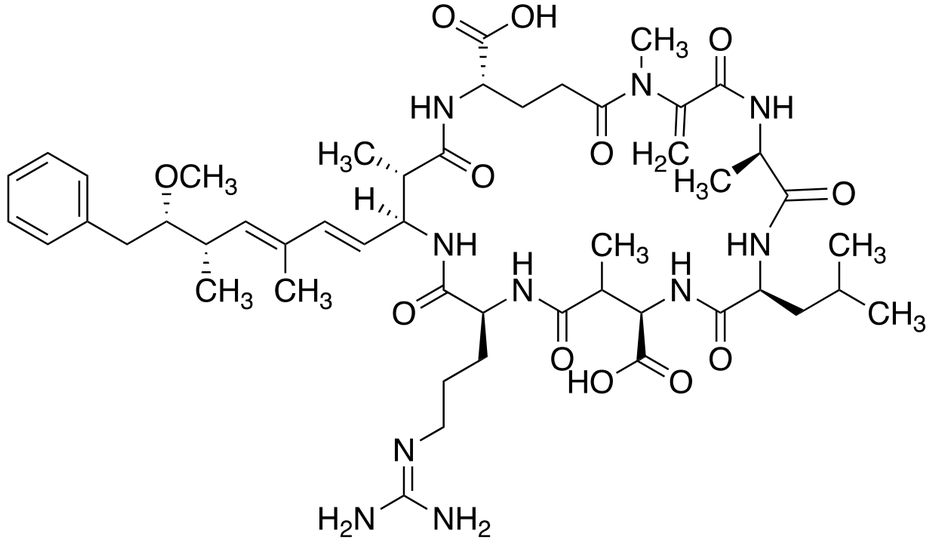

MC-LR

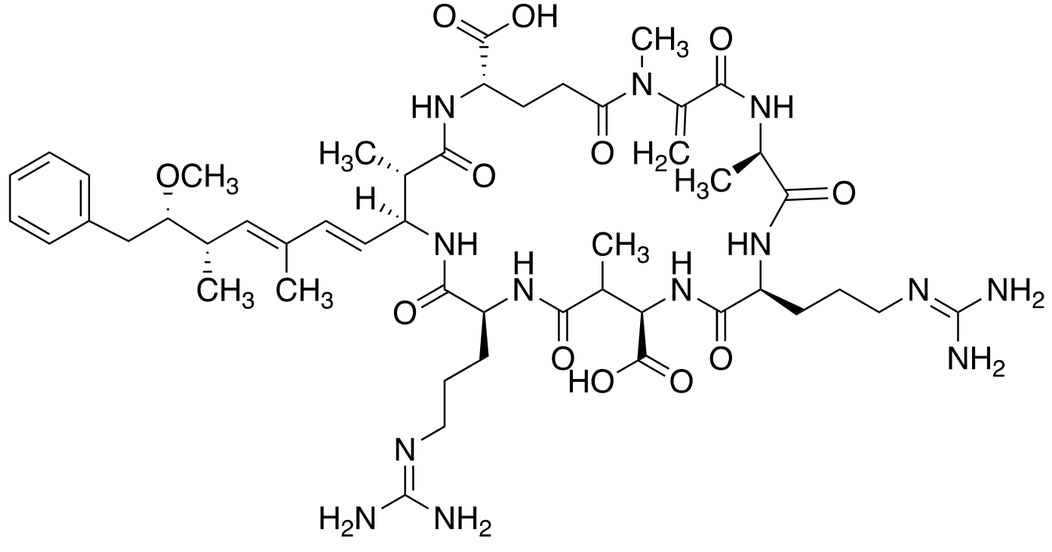

MC-RR

Figure 3
Click here to download Figure: Figure 3.pptx

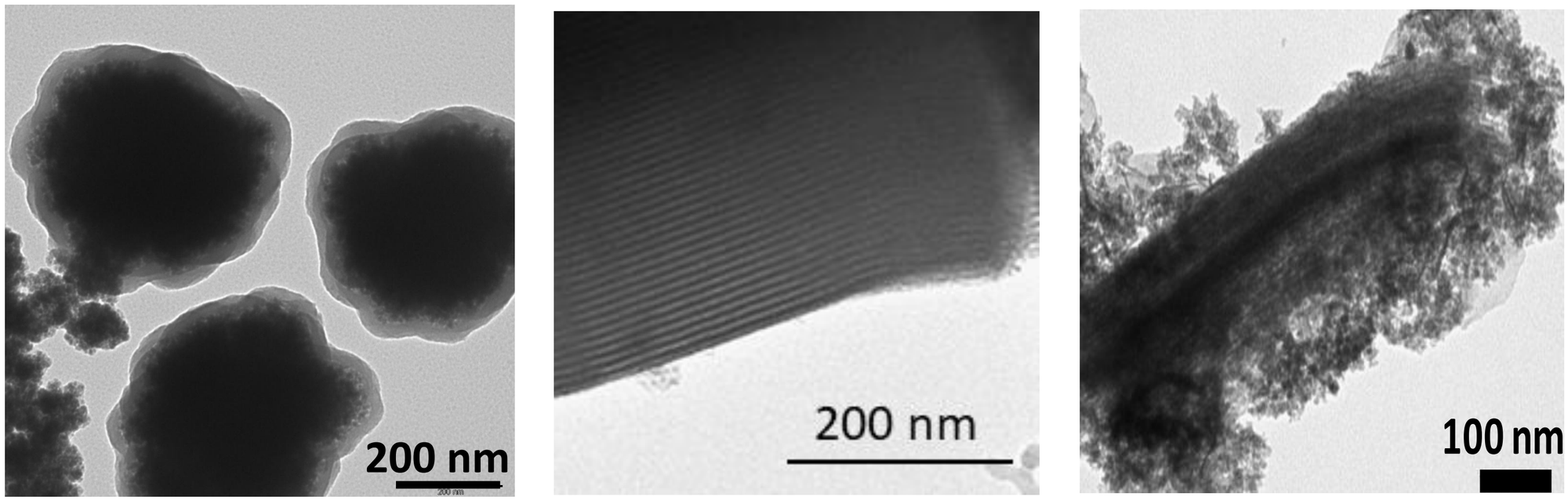

A B C

Figure 4

Click here to download Figure: Figure 4.pptx

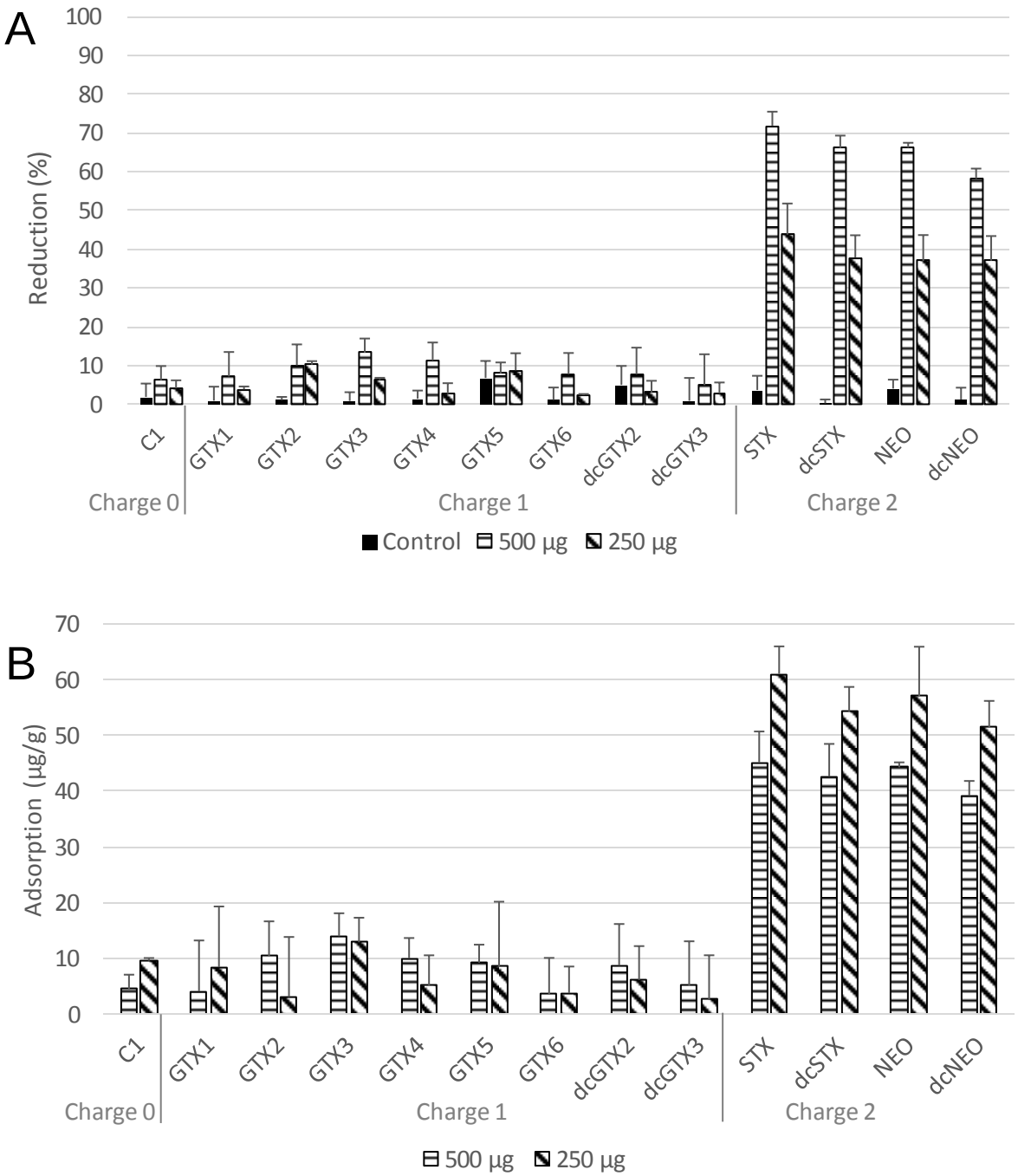

Figure 5

Click here to download Figure: Figure 5.pptx

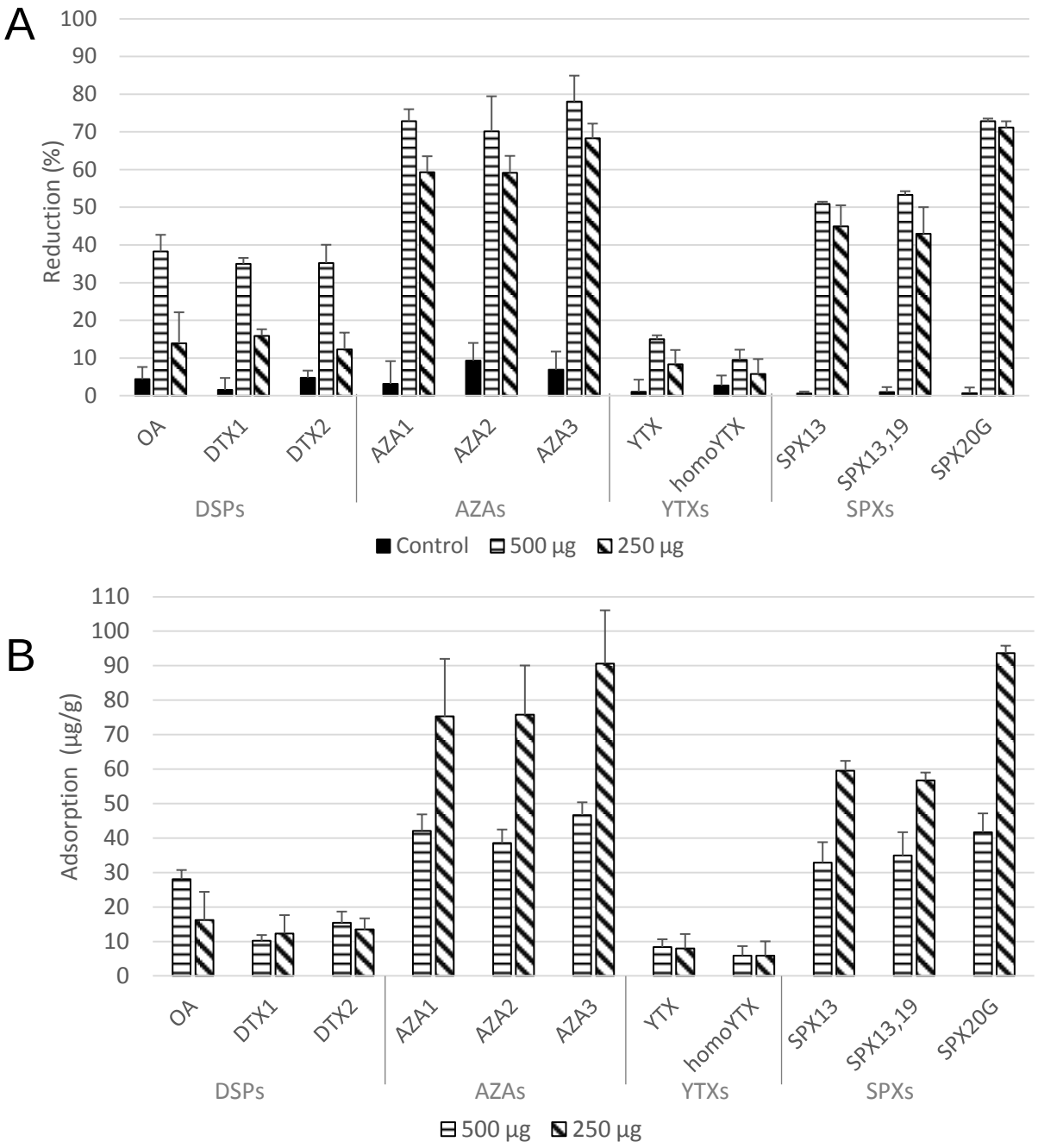

Figure 6

Click here to download Figure: Figure 6.pptx

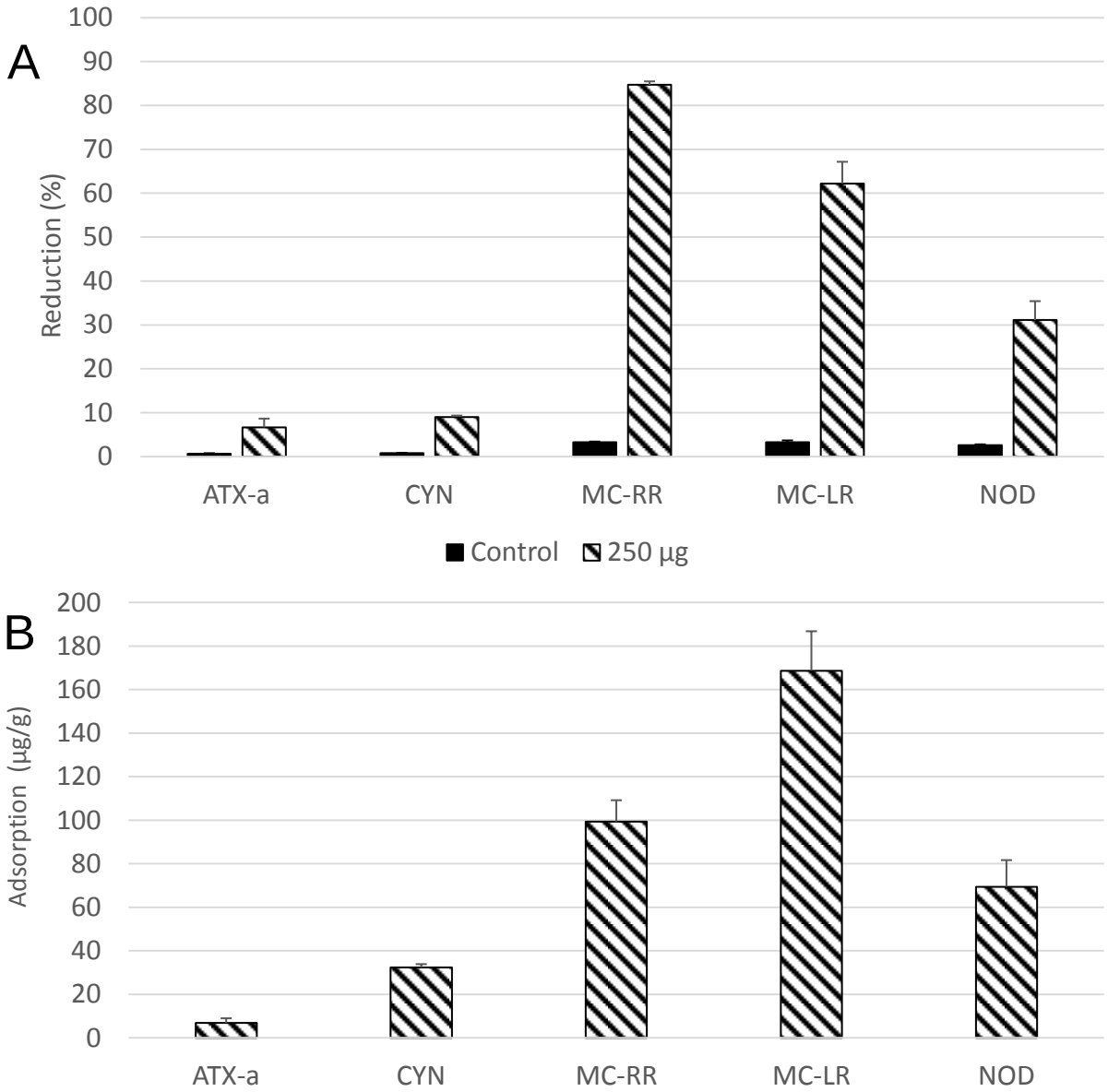

Figure 7

Click here to download Figure: Figure 7.pptx

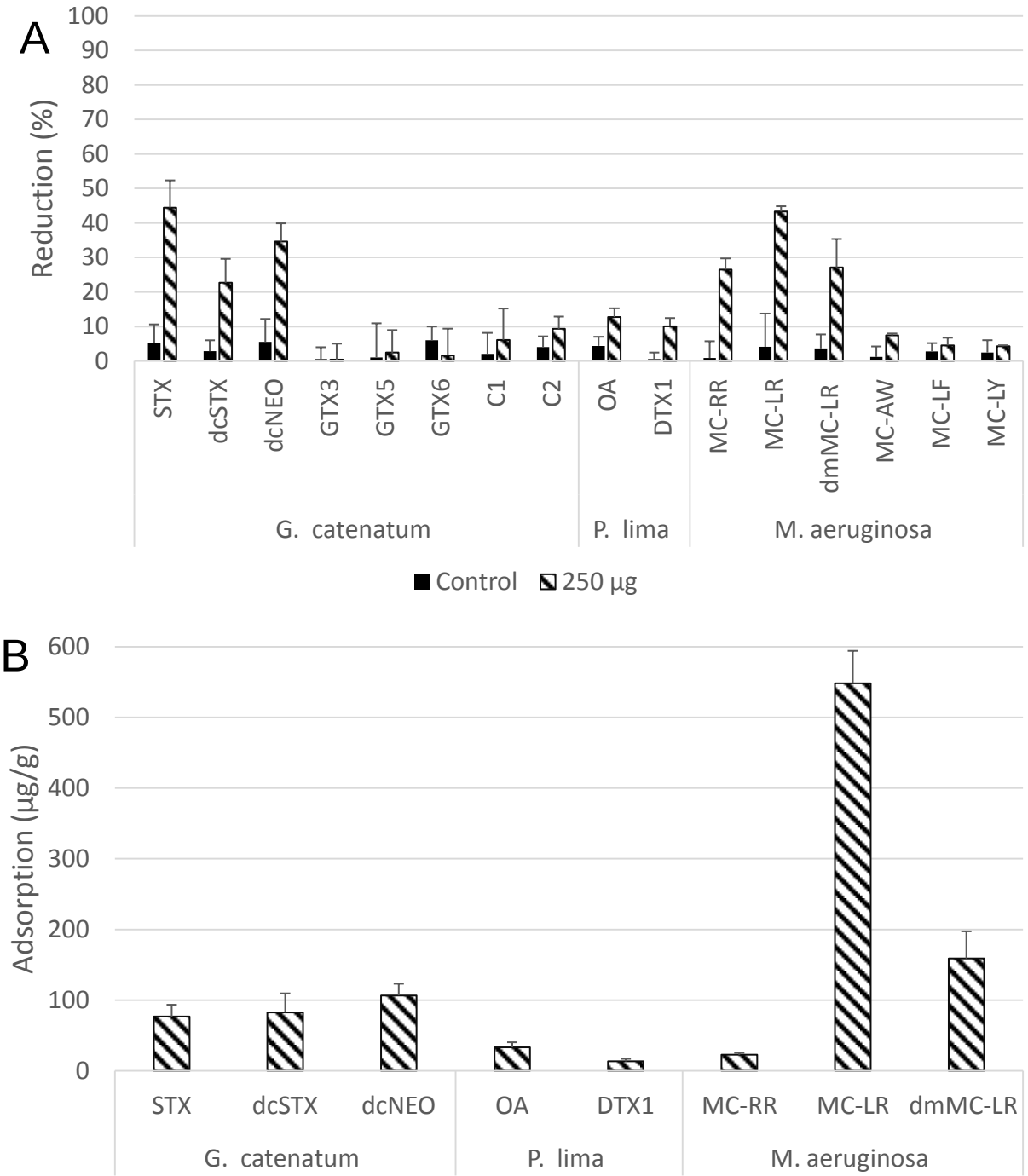

Figure Captions

Fig. 1. Chemical structure of marine toxins.

Fig. 2. Chemical structure of freshwater toxins.

Fig. 3. Transmission electron microscopy images of m-Fe_3O_4@C (A), mesoporous-Si@ Fe_3O_4 -NPs (B) and inner channels arrangement of mesoporous-Si nanostructures(C).

Fig. 4. Capacity of nanoparticles to adsorb hydrophilic marine toxins. (A) Adsorption expressed as percentage of toxin removed from solutions containing 20 µg/L of each toxin after incubation with nanoparticles for 60 min. Control solutions without particles addition (dark columns), solutions treated with 500 µg of nanoparticles (horizontal stripes columns) and solutions treated with 250 µg of nanoparticles (diagonal stripes columns). (B) Data from A expressed as µg of toxin removed by gram of carbon nanoparticles.

Fig. 5. Capacity of nanoparticles to adsorb lipophilic marine toxins. (A) Adsorption expressed as percentage of toxin removed from solutions containing 20 µg/L of each toxin after incubation with nanoparticles for 60 min. Control solutions without particles addition (dark columns), solutions treated with 500 µg of nanoparticles (horizontal stripes columns) and solutions treated with 250 µg of nanoparticles (diagonal stripes columns). (B) Data from A expressed as µg of toxin removed by gram of carbon nanoparticles.

Fig. 6. Capacity of nanoparticles to adsorb freshwater toxins. (A) Adsorption expressed as percentage of toxin removed from solutions containing 50 ng/mL of MC-LR and CYN, 25 ng/mL of ATX-a and NOD, as well as 12.5 ng/mL of MC-RR, after incubation with nanoparticles for 60 min. Control solutions without particles addition (dark columns), and

solutions treated with 250 µg of nanoparticles (diagonal stripes columns). (B) Data from A expressed as µg of toxin removed by gram of carbon nanoparticles.

Fig. 7. Capacity of nanoparticles to adsorb toxins from media with toxin-producing microorganisms. (A) Adsorption expressed as percentage of toxin removed from *Gymnodinium catenatum*, *Prorocentrum lima*, or *Microcystis aeruginosa* cultures after incubation with nanoparticles for 60 min. Control solutions without particles addition (dark columns), and solutions treated with 250 µg of nanoparticles (diagonal stripes columns). (B) Data from A expressed as µg of toxin removed by gram of carbon nanoparticles.

***Credit Author Statement**

Jesús M. González-Jartín: Investigation, Writing - Original Draft **Lisandra de Castro Alves**: Investigation, Writing - Original Draft **Amparo Alfonso**: Methodology, Writing - Review & Editing **Y. Piñeiro**: Methodology **Susana Yáñez Vilar**: Writing - Review & Editing **Inés Rodríguez**: Investigation, Validation **Manuel González Gomez**: Investigation **Zulema Vargas Osorio**: Investigation **María J. Sainz**: Investigation **Mercedes R. Vieytes**: Investigation **J. Rivas**: Conceptualization, Funding acquisition **Luis M. Botana**: Conceptualization, Funding acquisition, Supervision